Modelling and Prediction of the Effect of Cutting Strategy on Surface Generation in Ultra-precision Raster Milling

Sujuan Wang[a], Xin Chen[a], Sandy To[ab], Xindu Chen [a], Qiang Liu[a], Jiangwen Liu[a,*]

[a]Guangdong Provincial Key Laboratory for Micro/Nano Manufacturing Technology and Equipment, School of Electromechanical Engineering, Guangdong University of Technology, Guangzhou, China; [b]State Key Laboratory in Ultra-precision Machining Technology, Department of Industrial and Systems Engineering, The Hong Kong Polytechnic University, Kowloon, Hong Kong

*Corresponding author

Abstract: This paper studies the effect of cutting strategy on surface generation in ultra-precision raster milling (UPRM). By adding the influences of shift length and tool-interference on surface generation, a holistic surface roughness prediction model is built which takes into account the effect of cutting parameters, tool path generation, geometry parameters of diamond tool, the size of the workpiece and machine characteristics. The optimal shift ratio can be achieved by changing factors involved in developing cutting strategy to improve surface quality without decreasing machining efficiency. Conditions for the presence of tool-interference in UPRM are presented. Based on the holistic surface generation model, an integrated system is developed to automatically generate the numerical control (NC) program, and predict surface quality and machining efficiency. A series of cutting experiments has been conducted to verify the proposed surface generation model and test the performance of the integrated system. The experimental results agree well with the predicted results from the model and the integrated system.

Keywords: cutting strategy; surface generation; ultra-precision raster milling (UPRM); surface roughness

1. INTRODUCTION

Nowadays, freeform optics are becoming more popular for various advanced optics applications, which include printing, scanning, head-up displays and ophthalmic. However, the fabrication of freeform optics is difficult and time-consuming because of the complexity of the profile and the requirement for high quality. The surface quality is vital for the functionality and performance of the product (Benardos and Vosniakos 2003).

Ultra-precision raster milling (UPRM) with single crystal diamond tools can directly produce freeform surfaces with sub-micrometric form accuracy and nanometric surface finishing. However, the machining efficiency of UPRM is relatively low. The milling process becomes notoriously time-consuming when machining large freeform surfaces, such as freeform reflectors and freeform headlights in the automotive industry. At present, the control on surface quality still relies on a traditional trial and error approach which is time-consuming and uneconomical. Therefore, it is necessary to find an efficient way to produce high quality products by raster milling which indicates that, a better understanding on surface generation and a precise surface roughness prediction model are much needed in UPRM.

In the last few decades, lots of researches have been conducted on building surface

generation model by studying the factors affecting surface roughness in conventional machining, such as turning (Mital and Mehta 1988, Lin and Chang 1998, Abouelatta and Madl 2001), end milling (Kline et al. 1982, Omar et al. 2007, Fan and Loftus 2007, Li and Feng 2004), face milling (Baek et al. 1997), and high speed machining (Ozcelik and Bayramoglu 2006, Lee 2003, Luis et al. 2002). The factors being considered in these surface generation models include cutting parameters (i.e. spindle speed, feed rate), cutter geometry, tool wear, cooling strategy, spindle error motion and machine characteristics. However, all these surface generation models are unsuitable for ultra-precision machining, since the material removal mechanism and the chip formation of ultra-precision machining is radically different from conventional machining.

Recently, some researchers have focused on the study of surface generation model in single point diamond turning (SPDT) (Lee and Cheung 2001, To et al. 2001, Wang et al. 2013, Chen and Zhao 2015, Huang and Liang 2015). Nevertheless, the surface generation mechanism of raster milling is much more complex than that of SPDT, therefore the surface generation model of SPDT is not applicable for raster milling. A few recent studies have been found on UPRM for the applications of raster milling in the fabrication of high quality freeform surface (Cheung et al. 2006, Cheng et al. 2008, Wang et al. 2014, To and Zhang 2015) and the effect of material elastic recovery on the surface roughness (Wang et al. 2012, 2013). However, their theoretical models for surface roughness prediction are over simplified and have not considered the details about the tool paths, materials removal mechanisms, and their effect on the generation of 3D surface topography of the machined surfaces.

In this paper, a comprehensive 3D surface generation model is developed by considering the effects of shift length and tool-interference on surface generation in UPRM. Moreover, the quantitative relationship between cutting strategy and surface quality in UPRM is presented. Factors taken into consideration in the kinematic model of surface roughness prediction include tool path generation (TPG), cutting parameters, tool geometry, machine feed rate module and workpiece size. An optimization method for shift ratio is built by studying the effect of cutting strategy on shift length. A model-based integrated system is developed to select the cutting parameters, planning tool paths and automatically generate NC program for UPRM with the function of predicting the total machining time and surface roughness. The prediction model and the performance of the integrated system are verified by cutting experiment.

2. ULTRA-PRECISION RASTER MILLING

The ultra-precision freeform machine (Freeform 705G from Precitech, USA) can perform five axes of motions simultaneously which include three linear motions along the X_M, Y_M, and Z_M axes and two rotational motions using the B and C axes, respectively. Fig.1 (a) shows the configuration of the ultra-precision freeform machining system for UPRM. A single diamond tool is mounted on the spindle and the workpiece is set on the machine table. In raster milling process, the diamond tool in the spindle rotates around the spindle and linearly moves along Y_M-axis while the workpiece on the table makes linear movement along X_M-axis and Z_M-axis.

Fig.1 (a) the configuration of UPRM; (b) horizontal cutting strategy

When machining surface using raster milling process, the X_M-axis or Y_M-axis is usually selected as the feed direction which leads to two possible cutting strategies namely horizontal cutting and vertical cutting. In horizontal cutting (Fig.1 (b)), the feed direction is parallel to

X_M-axis and the raster direction is along the Y_M-axis and the Z_M-axis controls the contour to achieve the desired surface profile. Vertical cutting is done by changing the functions of the Y_M-axis and the X_M-axis. In Fig.1 (b), the distance between the tool tip and spindle center is called the swing distance (L) and the radius of the arc in the tool tip is called as the tool nose radius or tool tip radius (r).

3. DEVELOPMENT OF CUTTING STRATEGY

Cutting strategy in this study is the methodology to schedule the relative movement between the diamond tool and the workpiece by considering the effects of tool geometry, the material properties and geometry of workpiece, the surface generation mechanism and machine feed rate module on surface roughness. The development of cutting strategy involves in tool path generation (TPG) and the selection of cutting parameters (Fig.2). TPG in milling includes four main steps: the selection of feed direction, the confirmation of the tool path topology, the tool path linking method and path-interval. In UPRM, the main cutting parameters include spindle speed, cutting feed rate, rapid feed rate and depth of cut. Following this, numerical control (NC) program can be generated for the actual machining and surface roughness of the machined workpiece can be predicted to compare with the required surface quality.

Since the milling process is a 'point' tracing process where the diamond tool moves along a sequence of cutter contact (CC) points to achieve the desired surface (Marshall and Griffiths, 1994), the tool path topology in milling is the pattern of tracing or scanning during machining, which are classified into four types: serial-patterns, radial-patterns, strip-patterns and contour-patterns. In the present study, to simplify the programming task, the serial pattern is selected to plan tool paths for UPRM.

Fig.2 The development of cutting strategy for UPRM

Tool path linking method is generally classified into two types, i.e. one way (Fig. 3) and zig-zag. The one way method contains retreats in Z_M-axis direction for each tool path, while the zig-zag method has no any retreat in Z_M-axis direction expect for the first step and the last one. In Fig.3, l_P_j is the path-interval of the jth step; $h^C{}_j$ is the clearance height of the jth step; $l^e{}_j$ and $l^r{}_j$ refer to the entry and retreat distance of the jth step, respectively. In the actual machining process, the four parameters are kept constant, that is, $l\_P_j = l\_P_{j+1} = l\_P$, $h^C{}_j = h^C{}_{j+1} = h^C$, $l^e{}_j = l^e{}_{j+1} = l^e$, $l^r{}_j = l^r{}_{j+1} = l^r$. F_R and F_C are the rapid and cutting feed rate, respectively (mm/min). To improve machining efficiency, rapid feed rate (F_R) is generally set to be larger than the cutting feed rate (F_C). The presences of the clearance height, entry and retreat distances aim at making sure of machining safety.

Fig.3 The one way tool path linking methods

4. SURFACE GENERATION MECHANISM

For the development of an effective cutting strategy, one of main concerns is to have a larger feed rate and a larger path-interval since the increases of feed rate and path-interval can

help to improve machining efficiency. However, large feed rate and path-interval will results in a high surface roughness, therefore the two parameters should be well scheduled to make sure scallop heights within an allowable limit so as to satisfy the desired surface quality.

4.1. Pattern of surface topography

In UPRM, the diamond tool removes materials by making discontinuous contacts with the workpiece. This kind of material removal mechanism generates patterns on the machined surface. Fig. 4 (a) and (b) show two different scenarios of the generation of the patterns. They clearly indicate that the existence shift length (Δl_j) changes the patterns of the generated surface topography. Suppose $\overline{t}_j$ is the time that the diamond tool takes to finish one step and T_{circle} is the period of the tool rotation ($T_{circle} = 1/S$), the shift length (Δl_j) can be represented as:

$$\Delta l_j = MOD(\frac{\overline{t}_j}{T_{circle}}) \times T_{circle} \times F_C = MOD(\frac{\overline{t}_j}{T_{circle}}) \times f \quad (1)$$

where, the *MOD* function returns the remainder after a number is divided by a divisor. f is the feeding length per revolution: $f = F_C / S$. S is spindle speed (rpm). The shift ratio (η_j) in this study is defined as the ratio of shift length (Δl_j) to the feeding length per revolution (*f*): $\eta_j = \Delta l_j / f$.

Fig. 4 Patterns of surface topography for the: (a) absence of shift (b) existence of shift.

4.2. Calculation of shift length

From Eq. (1), the shift length depends on the feeding length per revolution (f), spindle speed (*S*) and the time ($\overline{t}_j$) used in one step. From Fig. 3, the time ($\overline{t}_j$) is affected by the tool path length of one step and the real feed rate for each cutting, which largely relies on the machine characteristics, such as the power of the motion axes used, the maximum acceptable accelerations and speeds. The ultra-precision machine (Fig.1 (a)) utilizes G10 mode to establish the standard acceleration and deceleration time setting for axes in the NC program. In this mode, any slides or rotary axes are accelerated or decelerated to the next position within 10ms. Fig. 5 show the feed rate profiles of machine axes in horizontal cutting, and vertical cutting only requires a shift of the feed rate profiles of the X_M-axis with those of the Y_M-axis. In Fig 5, the acceleration time and the deceleration time are equal to 10ms ($t_0 = 10$ ms). The time($\overline{t}_j$) used in one path between the *j*th and the (*j*+1)th step can be calculated:

$$\overline{t}_j = ({t^C}_j + \frac{60(l^e + l^r)}{F_C} + \frac{1}{2}t_0) + {t^R}_j = (\frac{60(l_j + l^e + l^r)}{F_C} + \frac{1}{2}t_0) + {t^R}_j \quad (2)$$

where, ${t^C}_j$ is the cutting time and represents the time used in the *j*th tool path where the diamond tool removes materials from the workpiece. ${t^R}_j$ refers to the time used to finish the rapid motions for the one way method:

$${t^R}_j = \frac{3t_0}{2} + \frac{120({h^C}_j + a_{ep}) + 60\sqrt{l\_P^2 + (l_j + l^e + l^r)^2}}{F_R} \quad (3)$$

Fig.5 Real feed rates of machine axes in horizontal cutting

From Eqs.(1)-(3), the deterministic model of the shift length has been proposed and the shift length is described as the function of cutting parameters (cutting feed rate, spindle speed, depth of cut and rapid feed rate), TPG (entry and retreat distance, clearance height and path-interval), the size of the workpiece and the acceleration and deceleration time of ultra-precision machine. This indicates that, the shift length can be well controlled to achieve a better surface roughness in UPRM by developing an optimal cutting strategy. In the machining process, the cutting feed rate F_C and the rapid feed rate F_R are kept constant, therefore, $\overline{t}_j = \overline{t}_{j+1} = \overline{t}$. Referring to Eq.(1) and Eq.(2), $\Delta l_j = \Delta l_{j+1} = \Delta l$; $\eta_j = \eta_{j+1} = \eta; (j = 1, 2\cdots, n)$.

4.3. Effect of shift length on surface generation

The existence of shift length makes an important effect on surface finishing in UPRM, in this study, which is named as 'shift effect'. The existence of shift length generates unparallel surface topography patterns on the machined surface which results in uneven surface profiles in raster direction by generating a shift height (Δhp_j) along the Z_M-axis direction, as shown in Fig.6. The shift height (Δhp_j) in raster direction due to the existence of shift length can be described as:

$$\begin{cases} \Delta hp_1 = 0 \\ \Delta hp_j = \sqrt{R_1^2 - ((j-1)\Delta l)^2} - \sqrt{R_1^2 - (j \cdot \Delta l)^2}; j = 2, \cdots, u \\ \Delta hp_j = \sqrt{R_1^2 - ((j-1) \cdot \Delta l)^2} - \sqrt{R_1^2 - (f - j \cdot \Delta l)^2}; j = u+1, \cdots, N \end{cases} \quad (4)$$

where, R_1 in horizontal cutting refers to swing distance (L), while in vertical cutting, R_1 is tool nose radius (r). $u = INT(1/2\eta)$; η is the shift ratio. The INT function returns the *integer* portion of a number.

Fig.6 Generation of shift height in raster direction due to the existence of shift length

4.4. Effect of tool-interference on surface generation

From Fig. 4, the generated surface topography pattern in UPRM relies on the relationships between the feeding length per revolution (*f*), the path-interval (*l_P*), the shift length and the contact lengths (*LF*, *LP*) in feed direction and raster direction. As the feeding length per revolution and path-interval meet: $f \geq LF/2$ and $l\_P \geq LP/2$, the formation of the surface roughness topography profile is clear and regular. Therefore, for large feeding length per revolution (*f*) and large path-interval (*l_P*), the diamond tool cuts sequentially and individually for each revolution which is referred to as the 'non-interference' in this study.

However, in ultra-precision machining process, a high spindle speed and a fine feed rate together with a small path-interval are usually adopted to ensure the desired high quality. When the shift length is zero, under the small feeding length per revolution and path-interval, the surface topography pattern remains clear and regular as shown in Fig. 7(a). On the other hand, in Fig.7 (b), for the case of existing shift length in feed direction, that is, $\Delta l \neq 0$, the small values of f and l_P result in irregular surface topography patterns on the machined surface since some areas left by the previous cuttings are removed by the preceding several cuttings, which referred to as the 'tool interference' in this study.

Fig.7 Surface topography patterns under small values of feeding length and path-interval: (a) in the absence of shift length; (b) in the existence of shift length

The conditions for the presence of tool-interference in feed direction can be divided into two parts: (1) $\Delta l \neq 0$; (2) $l\_P < \sqrt{2(R_2 - R_1)(R_1 - \sqrt{R_1^2 - \frac{f^2}{4}}) + \frac{f^2}{4}}$. Meanwhile, the conditions for tool-interference shown in raster direction include: (1) $\Delta l \neq 0$; (2) $l\_P < \sqrt{2(R_2 - R_1)(R_1 - \sqrt{R_1^2 - \Delta l^2}) + \Delta l^2}$. For horizontal cutting, R_1 refers to the swing distance (L) and R_2 is the tool nose radius (r); while for vertical cutting, R_1 is the tool nose radius (r) and R_2 represents the swing distance (L). This infers that, the presence of tool-interference is dependent on the cutting strategy and tool geometry as well as the existence of shift length. The investigation on the scallop generation in UPRM therefore is divided into three parts: (1) shift length is zero ($\Delta l = 0$); (2) $\Delta l \neq 0$ and no tool-interference; (3) $\Delta l \neq 0$ with tool-interference.

5. SCALLOP GENERATION MECHANISM

5.1. Feed-interval and path-interval scallop height

In UPRM, the resultant surface error is a combination of the errors in the feed and path-interval directions. The scallop heights in feed and raster directions are called the feed-interval and path-interval scallops, respectively. Fig. 8 presents the calculation model of feed-interval and path-interval scallop heights when shift length is equal to zero. The theoretical

models of the feed interval scallop height (h_f) and the path-interval scallop height (h_p) are shown in the following equations:

$$\begin{cases} h\_f = R_1 - \sqrt{R_1^{\,2} - \dfrac{f^2}{4}} \\ h\_p = R_2 - \sqrt{R_2^{\,2} - (\dfrac{1}{2} l\_P)^2} \end{cases} \tag{5}$$

Fig.8 The theoretical scallop height calculation model in (a) feed direction, (b) raster direction

The maximum peak-to-valley heights (R_{t_feed}, R_{t_raster}) in feed direction and raster direction are equal to the scallop heights in the two directions:

$$\begin{cases} R_{t\_feed} = R_1 - \sqrt{R_1^{\,2} - \dfrac{f^2}{4}} \\ R_{t\_raster} = R_2 - \sqrt{R_2^{\,2} - (\dfrac{1}{2} l\_P)^2} \end{cases} \tag{6}$$

5.2. Effect of shift length on scallop heights

Fig.9 presents the calculation model of path-interval scallop height under the consideration of shift effect. It shows that, the path-interval scallop height ($h\_p'_{i,j}$) between the *j*th and (*j*+1)th steps not only depends on tool geometry, cutting parameters but also is affected by the generated shift height in raster direction:

$$\begin{cases} j = 1, \cdots u-1 \Rightarrow h\_p'_{i,j} = \sum_{k=1}^{j} \Delta hp_k + R_2 + \dfrac{1}{2}(\Delta hp_{j+1} - \Delta hp_j) - \sqrt{\dfrac{R_2^{\,2}}{1 + (\dfrac{\Delta hp_{j+1} - \Delta hp_j}{l\_P})^2} - \dfrac{l\_P^2}{4}} \\ h\_p'_{i,u} = \sum_{k=1}^{u+1} \Delta hp_k + R_2 + \dfrac{1}{2}(\Delta hp_{u+1} - \Delta hp_u) - \sqrt{\dfrac{R_2^{\,2}}{1 + (\dfrac{\Delta hp_{u+1} - \Delta hp_u}{l\_P})^2} - \dfrac{l\_P^2}{4}} \end{cases} \tag{7}$$

where, the factor *u* is the same with that in Eq. (4).

Fig.9 Effects of shift length on path-interval scallop height without tool-interference

The maximum peak-to-valley height (R_{t_raster}) in raster direction therefore can be represented as follows:

$$R_{t\_raster} = \sum_{k=1}^{u+1} \Delta hp_k + R_2 + \frac{1}{2}(\Delta hp_u - \Delta hp_{u+1}) - \sqrt{\frac{R_2^{\,2} \times l\_P^2}{l\_P^2 + \Delta hp_u^{\,2}} - \frac{l\_P^2}{4}}$$

$$= R_2 + (R_1 - \sqrt{R_1^{\,2} - (u+1)^2 \cdot \Delta l^2}) + \frac{1}{2}(\sqrt{R_1^{\,2} - u^2 \cdot \Delta l^2} - \sqrt{R_1^{\,2} - (f - (u+1) \cdot \Delta l)^2}) \quad (8)$$

$$- \sqrt{\frac{R_2^{\,2} \cdot l\_P^2}{l\_P^2 + (\sqrt{R_1^{\,2} - u^2 \cdot \Delta l^2} - \sqrt{R_1^{\,2} - (f - (u+1) \cdot \Delta l)})^2} - \frac{l\_P^2}{4}}$$

And the widths of each generated surface profile in the raster direction ($Wp_{i,j}$ and $Wp'_{i,j}$) are changed due to the existence of shift length:

$$\begin{cases} Wp'_{i,j} = \frac{1}{2} l\_P - \sqrt{\frac{R_2^{\,2} \cdot \Delta hp_j^{\,2}}{\Delta hp_j^{\,2} + l\_P^2} - \frac{\Delta hp_j^{\,2}}{4}} \\ Wp_{i,j} = \frac{1}{2} l\_P + \sqrt{\frac{R_2^{\,2} \cdot \Delta hp_{j+1}^{\,2}}{\Delta hp_{j+1}^{\,2} + l\_P^2} - \frac{\Delta hp_{j+1}^{\,2}}{4}} \end{cases} \quad (9)$$

5.3. Effect of tool-interference on scallop heights

Fig.10 illustrates the tool-workpiece contact loci when tool-interference exists in feed direction. From this figure, it can be found that, a small value of path-interval (l_P) generates a shift height (Δhf_j) in feed direction between the jth step and the (j-1)th step: $\Delta hf_j = \sqrt{R_2^{\,2} - (j-1)^2 l\_P^2} - \sqrt{R_2^{\,2} - (j \cdot l\_P)^2}$ ($j = 1, \cdots, N$). When the shift height in feed direction is smaller than the feed-interval scallop height, that is, $\Delta hf_{j+1} < h\_f_{i,j}$, the materials left by the previous cuttings ($C_{i,j}, C_{i+1,j}$) will be removed by the following cuttings ($C_{i,j+1}$, $C_{i+1,j+1}$, $C_{i,j+2}$, $C_{i+1,j+2}$). Therefore, the actual generated feed-interval scallop height ($h\_f'_{i,j}$) by adding the influence of tool-interference can be confirmed as follows:

$$h\_f'_{i,j} = R_1 + \frac{1}{2}(R_2 - \sqrt{R_2^{\,2} - l\_P^2}) - \sqrt{\frac{R_1^{\,2}}{1 + (\frac{R_2 - \sqrt{R_2^{\,2} - l\_P^2}}{f(1-\eta)})^2} - \frac{f^2(1-\eta)^2}{4}} \quad (10)$$

The maximum peak-to-valley height (R_{t_feed}) in feed direction therefore is expressed as:

$$R_{t\_feed} = R_1 + \frac{R_2 - \sqrt{R_2^{\,2} - \delta^2 l\_P^2}}{2} - \sqrt{\frac{R_1^{\,2}}{1 + (\frac{R_2 - \sqrt{R_2^{\,2} - \delta^2 l\_P^2}}{f(1-\delta \cdot \eta)})^2} - \frac{f^2(1-\delta \cdot \eta)^2}{4}} \quad (11)$$

where, the factor (δ) depends on the tool geometry (L, r), path-interval, the feeding length and

shift ratio: $\delta = INT(MIN(\frac{\sqrt{2(R_2 - R_1)(R_1 - \sqrt{R_1^2 - \frac{f^2}{4}}) + \frac{f^2}{4}}}{l\_P}, \frac{1}{2\eta}))$. The *INT* function returns the *integer* portion of a number and the *MIN* function returns the smallest value from the numbers provided.

Fig.10 Effect of tool-interference on feed-interval scallop height generation

At the same time, the tool-interference in raster direction together with the existence of shift length affects the generation of path-interval scallop height (Fig.11). The maximum peak-to-valley height (R_{t_raster}) in the raster direction under the consideration of tool-interference and shift effect is:

$$R_{t\_raster} = R_2 + \frac{1}{2}(R_1 - \sqrt{R_1^2 - f^2(1-u\eta)^2}) - \sqrt{\frac{R_2^2}{1 + (\frac{R_1 - \sqrt{R_1^2 - f^2(1-u\eta)^2}}{u \cdot l\_P})^2} - \frac{(u \cdot l\_P)^2}{4}} \tag{12}$$

Fig.11 Effect of tool-interference on the path-interval scallop height generation

Because of the presence of tool-interference in raster direction, the widths of the generated surface profile ($Wp_{i,j}$ and $Wp'_{i,j}$) are changed as:

$$\begin{cases} Wp'_{i,j} = \dfrac{u \cdot l\_P}{2} - \sqrt{\dfrac{R_2^2}{1 + (\dfrac{u \cdot l\_P}{(R_1 - \sqrt{R_1^2 - (f - u\Delta l)^2})})^2} - \dfrac{(R_1 - \sqrt{R_1^2 - (f - u\Delta l)^2})^2}{4}} \\ Wp_{i,j} = \dfrac{u \cdot l\_P}{2} + \sqrt{\dfrac{R_2^2}{1 + (\dfrac{u \cdot l\_P}{(R_1 - \sqrt{R_1^2 - (f - u\Delta l)^2})})^2} - \dfrac{(R_1 - \sqrt{R_1^2 - (f - u\Delta l)^2})^2}{4}} \end{cases} \tag{13}$$

where, the factor (u) depends on the shift ratio: $u = ROUND(1/\eta, 0)$. The function *ROUND* (number, digits) returns a number rounded to a specified number of digits.

From previous studies, the concurrence of shift length and tool-interference decreases the values of R_{t_feed} and R_{t_raster}. Therefore, when developing cutting strategy, a well control on the relationship between the tool-interference, shift length and cutting parameters as well as TPG can be conducted to achieve a better surface finishing in UPRM.

5.4. Confirmation of the maximum peak-to-valley heights

According to the investigations on the scallop height generation mechanism in UPRM,

under different cutting conditions, the surface generation mechanism is different due to the influences of shift length and tool-interference. Fig.12 presents the process of calculating the maximum peak-to-valley (PV) height in feed direction and raster direction. It shows that, after the selections of cutting parameters, tool geometry and planning tool paths, shift length can confirmed: if shift length is zero, the PV heights only depend on tool geometry, feeding per revolution (*f*) and path-interval (l_P) in Eq. (6).

Fig.12 Flow chart of calculating the PV heights in UPRM

If shift length is not zero and the path-interval meets the conditions: $l\_P \geq \sqrt{2(R_2-R_1)(R_1-\sqrt{R_1^2-\frac{f^2}{4}})+\frac{f^2}{4}}$, there is no tool-interference in both feed direction and raster direction. Under these cutting conditions, the feed-interval scallop height is calculated by Eq.(6) and the path-interval scallop height is the function of tool geometry, path-interval and shift ratio (Eq.(8)).

If $l\_P < \sqrt{2(R_2-R_1)(R_1-\sqrt{R_1^2-\frac{f^2}{4}})+\frac{f^2}{4}}$, there is tool-interference in feed direction and therefore the PV height in feed direction is the function of feeding length per revolution, tool geometry and path-interval as well as shift ratio(Eq.(11)). When path-interval and shift length meets: $l\_P < \sqrt{2(R_2-R_1)(R_1-\sqrt{R_1^2-\Delta l^2})+\Delta l^2}$, tool-interference occurs in raster direction and the PV height in raster direction is also affected by feeding length per revolution and shift ratio besides tool geometry and path-interval (Eq. (12)).

6. KINEMATIC MODEL OF SURFACE ROUGHNESS PREDICTION

Fig.13 (a) and (b) present the three-dimensional (3D) surface generation models for the absence and existence of shift length. From these figures, the existence of shift length changes the positions and the number of the vertexes on the raster milled surface. Therefore, by adding the effects of shift length and tool-interference on surface generation, the maximum peak-to-valley height (R_t) of the raster milled surface is represented as:

$$R_t(L,r,f,l\_P,a_{ep},\eta) = R_1 + R_2 - \sqrt{R_1^2-\frac{f^2}{4}(1-2k\eta+k(k+1)(\eta^2+\frac{e^2 l\_P^2}{f^2}))^2} - \sqrt{R_2^2-\frac{l\_P^2}{4}(1-\frac{f^2(1-k\cdot\eta)(1-(k+1)\cdot\eta)\eta}{e^2 l\_P^2}-k(k+1)\eta)^2} \quad (14)$$

where, the parameters e is a ratio which is related to tool geometry and depth of cut: $e=\left(2R_1-a_{ep}\right)/\left(2R_2-a_{ep}\right)$; the factor *k* depends on the development of cutting strategy and tool geometry: $k=INT\left[\left(\eta f^2\right)/\left(\eta^2 f^2+e^2\cdot l\_P^2\right)\right]$. The *INT* function returns the integer portion of a number.

From Eq.(14), if $\Delta l = 0$, the maximum peak-to-valley height (R_t) of the machined surface is simplified as follows:

$$R_t(R_1, R_2, f, l\_P) = R_1 + R_2 - \sqrt{R_1^2 - \frac{f^2}{4}} - \sqrt{R_2^2 - \frac{l\_P^2}{4}} \tag{15}$$

When no tool-interference presents in feed direction and raster direction, the maximum peak-to-valley height (R_t) of the machined surface is the function of tool geometry (L, r), the feeding length per revolution (f), path-interval (l_P) and shift ratio (η):

$$R_t(L, r, f, l\_P, \eta, e) = R_1 + R_2 - \sqrt{R_1^2 - \frac{f^2}{4}} - \sqrt{R_2^2 - \frac{l\_P^2}{4}(1 - \frac{f^2 \cdot \eta(1-\eta)}{e^2 \cdot l\_P^2})^2} \tag{16}$$

Fig.13 The 3D surface roughness prediction model for (a) the absence of shift length; (b) the existence of shift length

According to Eqs.(15) and (16), the presence of shift length improves surface quality in UPRM. And the optimal shift ratio is dependent on the developed cutting strategy and tool geometry:

$$\eta_{op} = \sqrt{\frac{l\_P \cdot e}{f}(\frac{2}{\sqrt{3}} - \frac{l\_P \cdot e}{f})} \tag{17}$$

Eqs.(6)-(17) provide an important theoretical means for studying the effect of cutting strategy on surface roughness in UPRM. In the present study, a deterministic surface roughness prediction model is built for UPRM by considering the influences of shift length, cutting parameters, too geometry, TPG, the size of the workpiece and the machine characteristics on surface generation. Meanwhile, based on the developed surface roughness prediction model, the confirmation of the optimal shift ratio is proposed to achieve a better surface quality in UPRM.

7. IMPLEMENTATION AND EXPERIMENTAL VERIFICATION

7.1. The integrated system for developing cutting strategy

In previous parts, this paper has built a quantitative relationship between the cutting strategy and surface roughness in UPRM. The factors affecting surface roughness are considered in this paper including cutting parameters, tool geometry (tool nose radius, swing distance), and the size of the workpiece as well as the ac/deceleration time of machine. Based on these studies, an integrated system has been established for the development of cutting strategy in UPRM. Fig.14 shows the process of developing cutting strategy, generating NC program and predicting surface quality by using the integrated system. It can be found that, the system is composed of three core parts: simulation, prediction and automatic generation of NC program, as shown in Fig. 14. The system provides simulations for the machined surface profile and the generated tool paths and predicts the produced surface quality and the required machining time. The generated NC program can be directly input into the ultra-precision freeform machining system (Freeform 705G) to achieve the desired products. By using this system, the expensive and time consuming trial and error cutting tests can be minimized and the machining time can be customized.

Fig.14 Flow chart of the integrated system for UPRM

7.2. Verification of surface roughness prediction model

Cutting experiments are conducted on the 5-axis freeform machining system (Fig.1) to study the effect of cutting strategy on surface quality in UPRM. After machining, the machined samples were measured by an optical profile system (Wyko NT 8000) to measure the surface roughness. The measured results are compared with the predicted ones provided by the integrated system for three main objectives: firstly to test the performance of the developed system; secondly to verify the surface roughness prediction model presented in this study, and thirdly to demonstrate the importance of the consideration of the shift effect on surface roughness in UPRM.

The experiments were performed on aluminum alloy 6061 by using horizontal cutting and vertical cutting. Table 1 shows the cutting parameters and the geometrical parameters of the diamond tool. In this experiment, the cutting feed rate is changed from 50 mm/min to 400 mm/min while other cutting parameters are kept constant. Fig.15 (a) and (b) show the effects of cutting feed rate on surface roughness in horizontal cutting and vertical cutting respectively. The predicted results include two parts: one ignores the shift effect and the other one adding the shift effect on surface roughness prediction. And the measured surface profiles are shown in Fig. 15 for different cutting feed rates.

Table 1 Cutting parameters and the geometrical parameters of the tool

In Fig.15, by comparing the predicted results with the measured ones, it is found that, in horizontal cutting and vertical cutting, the predicted surface roughness adding shift effect is much more close to the measured results. This indicates that, shift length is an important factor affecting surface roughness in UPRM. Meanwhile, the predicted surface roughness by ignoring the effect of shift length is higher than that under the consideration of shift length, which infers the existence of shift length contributes to improving surface quality in UPRM.

Fig.15 Effects of cutting feed rate on the arithmetical mean roughness (R_a) in: (a) horizontal cutting; (b) vertical cutting

At the same time, in horizontal cutting, the measured surface roughness increases with the increasing cutting feed rate (Fig.15 (a)) while in vertical cutting, the effect of cutting feed rate on surface roughness is different. In Fig.15(b), as cutting feed rate increases from 50 mm/min to 300 mm/min, the surface roughness increases, however, when cutting feed rate increases from 300 mm/min to 400 mm/min, the achieved surface quality becomes better which is due to the influence of shift length on surface roughness in UPRM. The higher the cutting feed rate, the larger the improvement on surface quality induced by the existence of shift length.

Moreover, the improvement on surface quality due to the shift length in vertical cutting is larger than that in horizontal cutting. In Fig.15 (a), as cutting feed rate decreases from 400

mm/min to 50 mm/min, the largest improvement on surface quality in horizontal cutting is about 30nm(R_a); while in vertical cutting, the surface quality is improved nearly 500nm(R_a) in Fig.15(b). This is because of that, in vertical cutting, tool-interference is shown in raster direction which results in a larger improvement on the surface quality of the raster milled surface.

Especially, the measured surface quality in horizontal cutting is better than the predicted one when feed rate is smaller than 400mm/min, see Fig.15(a). The reason is that the material elastic recovery in ultra-precision machining improves the surface finishing (To, 2001; Wang, 2013), while the surface roughness prediction model proposed in this paper ignores the material effect on surface generation in UPRM. Moreover, when the feed rate increases from 50mm/min to 400mm/min, the deviation between the measured roughness and the predicted one with shift effect becomes smaller and smaller. It is because that the material's effect on surface generation becomes relatively insignificant as compared with the kinematic roughness under a larger feed rate (Wang, 2012)

7.3. Effects of shift ratio on surface roughness

The previous experimental results show that, the influence of shift length on surface roughness in vertical cutting is larger than that in horizontal cutting. Therefore, to study the influence of shift ratio on surface generation in UPRM, experiments are conducted to change entry distance to generate different shift ratios in vertical cutting when cutting feed rate is set to 300 mm/min. The tool geometry and other cutting conditions are presented in Table 1. Fig.16 presents the effects of shift ratio on surface roughness and surface profiles in vertical cutting.

Fig.16 Effects of shift ratio on surface roughness (Ra) in vertical cutting (F_C=300 mm min^{-1})

In Fig.16, the change of shift ratio generates different surface profiles in UPRM. Moreover, as shift ratio increases from 7.5% to 45%, the surface roughness firstly decreases then increases. The best surface finishing (R_a 25.21nm) is achieved when the shift ratio is 28%, which is close to the predicted optimal shift ratio (27.6%) calculated by Eq. (17). Meanwhile, when the entry distance is changed about 0.02mm which costs extra machining time less than 5.0ms, the shift ratio is changed from 15% to 28% and the surface quality is improved nearly 40nm (R_a). Therefore, this study makes contribution to improving surface quality without decreasing machining efficiency in ultra-precision raster milling process.

8. CONCLUSION

This paper presents a new surface generation model to study the effect of cutting strategy on surface generation in UPRM. By considering the influences of shift length and tool-interference on surface generation, the factors taken into consideration include cutting parameters, tool geometry, workpiece size, TPG and the ac/deceleration time of the ultra-precision machine. The calculation method of shift length is developed and conditions for the presence of tool-interference in UPRM are determined. The optimal shift ratio is found to be determined by the employed cutting strategy and tool geometry. This helps provide a new idea to achieve an optimal shift ratio so as to improve surface quality with a little increasing in the machining time.

Based on the proposed surface roughness prediction model, an integrated system has been developed to predict surface roughness and machining efficiency, and for the simulation of tool paths, the surface profile and NC program generation. Cutting experiments have also been conducted on a 5-axis freeform machine to verify the proposed surface roughness prediction model and test the developed system.

On the whole, the following conclusions can be drawn:

(i) the predicted surface roughness agrees well with the experimental results which indicates that the proposed kinematic surface roughness prediction model is more precise;

(ii) the shift length is an important factor affecting surface generation in UPRM;

(iii) the existence of shift length improves surface quality and the generation of shift length can be well controlled by developing cutting strategy;

(iv) the improvement on surface quality due to the existence of shift length in vertical cutting is larger than that in horizontal cutting;

(v) the optimal shift ratio is dependent on the developed cutting strategy and tool geometry, in this study, the optimal shift ratio for vertical cutting is about 28%;

(vi) the optimal shift ratio contributes to improve surface quality without decreasing machining efficiency.

The present study provides an important mean for a better understanding of the surface generation mechanism in UPRM. With the successful development of the kinematic surface roughness prediction model and the prediction method of optimal shift length, tool paths can be optimized and the surface quality of the raster milled surface can also be optimized without the need to conduct expensive and time consuming trial cutting tests. This can make the ultra-precision raster milling process more predictable and more efficient.

ACKNOWLEDGEMENTS

The authors would like to express their sincere thanks to the support of National Natural Science Foundation of China (no. 51205067) and Guangdong Innovative Research Team Program (no. 201001G0104781202). The authors would also like to thanks the support by Guangdong Natural Science Foundation (no.2015A030312008) and Guangdong Provincial Project (no. 2011A090200119).

REFERENCES

Abouelatta, O.B., J. Madl, 2001. Surface roughness prediction based on cutting parameters and tool vibrations in turning operations. *Journal of Materials Processing Technology*, 118, 269–277.

Baek, D.K., Ko, T.J. and Kim, H. S., 1997. A dynamic surface roughness model for face milling. *Precision Engineering*, 20, 171-178.

Benardos, P.G., Vosniakos, G.C., 2003. Predicting surface roughness in machining: a review. *International Journal of Machine Tools & Manufacture*, 43, 833–844.

Chen, J.Y. and Zhao, Q.L., 2015. A model for predicting surface roughness in single-point diamond turning. *Measurement*, 69, 20-30.

Cheng, M.N., Cheung, C.F., Lee, W.B., To, S., Kong, L.B., 2008. Theoretical and experimental analysis of nano-surface generation in ultra-precision raster milling. *International Journal of*

Machine Tools & Manufacture, 48, 1090–1102.

Cheung, C.F., Kong, L.B., Lee, W.B. and To, S., 2006. Modelling and simulation of freeform surface generation in ultra-precision raster milling. *Proceedings of the IMechE, Part B: Journal of Engineering Manufacture*, 220, 1787-1801.

Huang, C.Y. and Liang, R.G., 2015. Modeling of surface topography in single-point diamond turning machine. *Applied Optics*, 54(23), 6979-6985.

Fan, X. and Loftus, M., 2007. The influence of cutting force on surface machining quality. *International Journal of Production Research*, 45(4), 899–911.

Kline, W.A., DeVor, R.A. and Shareef, I.A., 1982. The prediction of surface geometry in end milling. *Journal of Engineering for Industry-Transactions of the ASME*, 104, 272-278.

Lee, E., 2003. Contour offset approach to spiral toolpath generation with constant scallop height. *Computer-Aided Design*, 35, 511-518.

Lee, W.B., Cheung, C.F., 2001. A dynamic surface topography model for the prediction of nano-surface generation in ultra-precision machining. *International Journal of Mechanical Sciences*, 43, 961-991.

Li, H. and Feng, H.-Y., 2004. Efficient five-axis machining of free-form surfaces with constant scallop height tool paths. *International Journal of Production Research*, 42(12), 2403-2417.

Lin, S.C., Chang, M.F., 1998. A study on the effects of vibrations on the surface finish using a surface topography simulation model for turning. *International Journal of Machine Tools and Manufacture*, 38, 763–782.

Luis N., Lacalle, Lopez de, Lamikiz, A., Sanchez, J.A., Arana, J.L., 2002. Improving the surface finish in high speed milling of stamping dies. *Journal of materials processing technology*, 123, 292-302.

Marshall, S. and Griffiths, J.G., 1994. A new cutter-path topology for milling machines. *Computer-Aided Design*, 26(3), 204-214.

Mital, A. and Mehta, M., 1988. Surface roughness prediction models for fine turning. *International Journal of Production Research*, 26, 1861–1876.

Omar, O.E.E.K., Wardany, T. El-, Ng, E., Elbestawi, M.A., 2007. An improved cutting force and surface topography prediction model in end milling. *International Journal of Machine Tools & Manufacture*, 47, 1263–1275.

Ozcelik, B., Bayramoglu, M., 2006. The statistical modeling of surface roughness in high-speed flat end milling. *International Journal of Machine Tools & Manufacture*, 46, 1395–1402.

To, S., Cheung, C.F. and Lee, W.B., 2001. Influence of material swelling on surface roughness in diamond turning of single crystals. *Materials Science and Technology*, 17, 102-108.

To, S. and Zhang, G.Q., 2014. Study of cutting force in ultra-precision raster milling of V-groove. *The International Journal of Advanced Manufacturing Technology*, 75(5-8), 967-978.

Wang, H., To, S., Chan, C.Y., 2013. Investigation on the influence of tool-tip vibration on surface roughness and its representative measurement in ultra-precision diamond turning.

International Journal of Machine Tools and Manufacture, 69, 20-29.

Wang, S.J., To, S., Chan, C. Y., Cheung, C. F., 2012. Effect of Workpiece material on surface roughness in ultra-precision raster milling. *Materials and Manufacturing Processes*, 27(10):1022-1028.

Wang, S.J., To, S., Cheung, C. F., 2013. An investigation into material-induced surface roughness in ultra-precision milling. *The International Journal of Advanced Manufacturing Technology*, 68:607–616.

Wang, S.J., To, S., Chen, X., Wang, H., Xia, H.J., 2014. A study of the fabrication of v-groove structure in ultra-precision milling. *International Journal of Computer Integrated Manufacturing*, 27(11): 986-996.

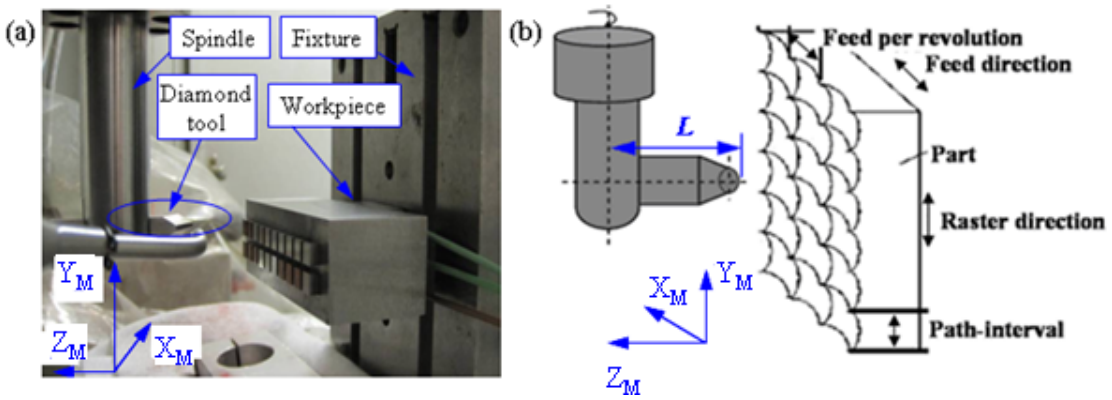

Figure1. (a) the configuration of UPRM; (b) horizontal cutting strategy

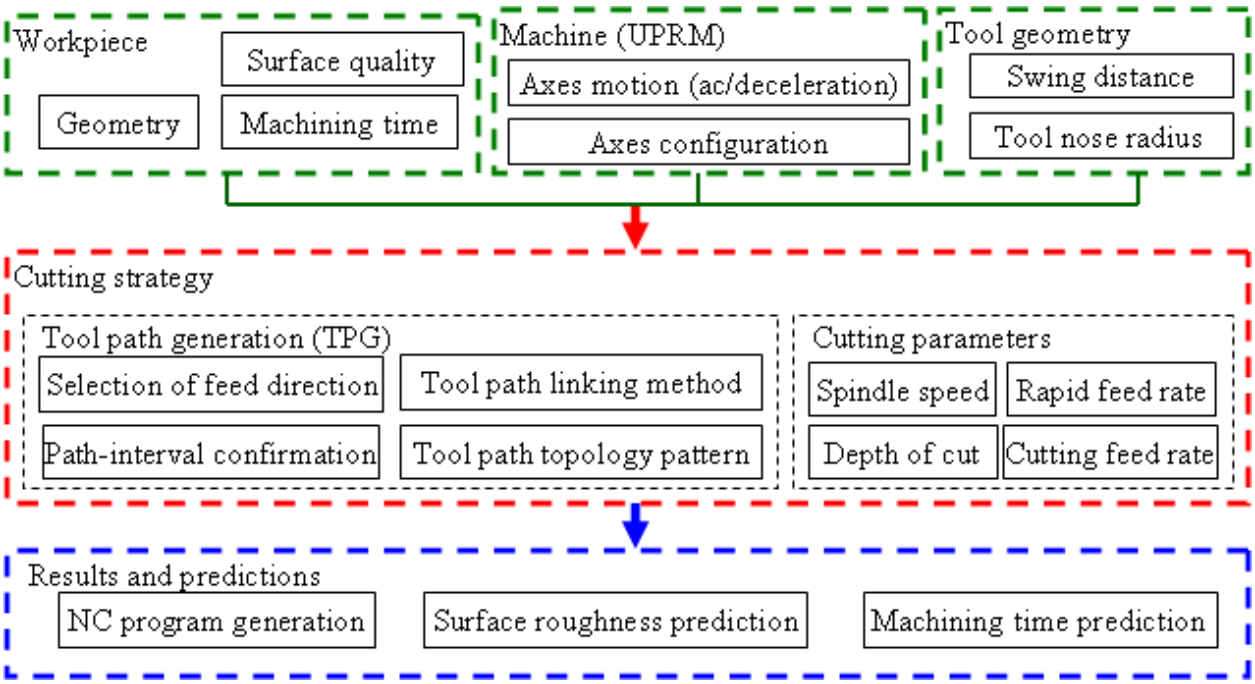

Figure 2. The development of cutting strategy for UPRM

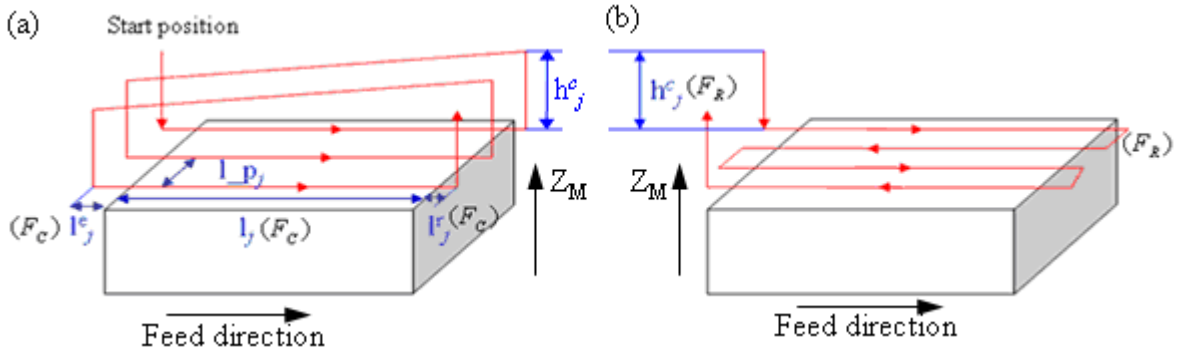

Figure 3. Tool path linking methods design: (a) one way, (b) zig-zag

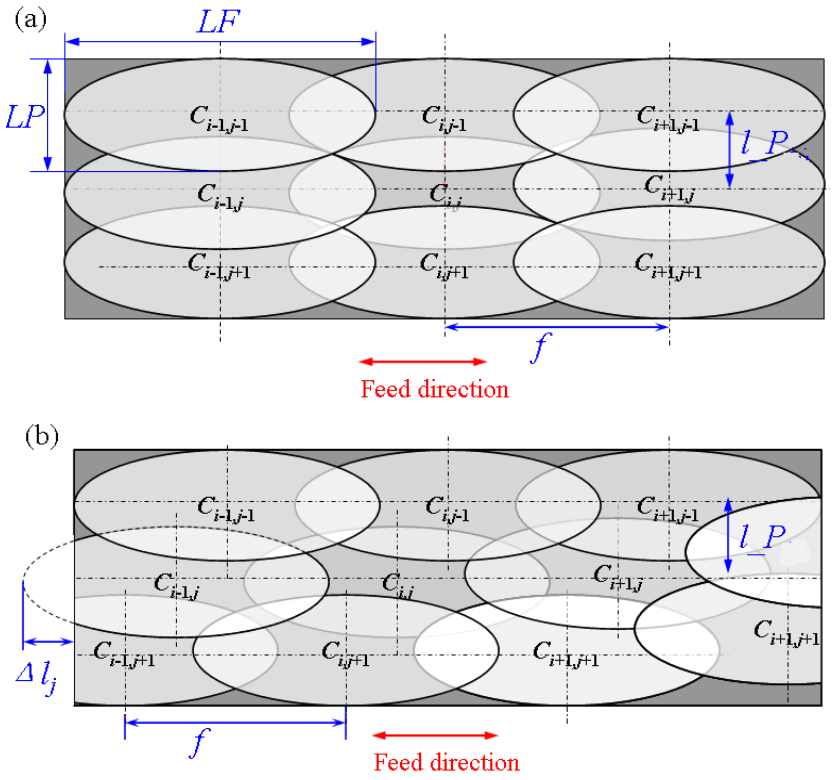

Figure 4. Patterns of surface topography for the: (a) absence of shift (b) existence of shift.

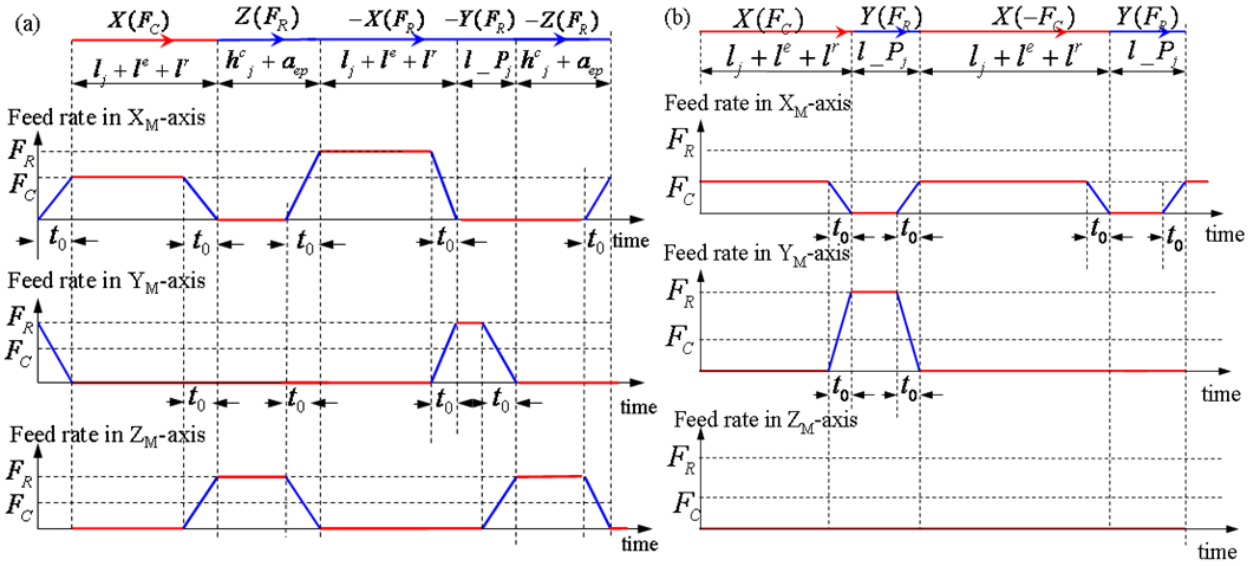

Figure 5. Real feed rates of machine axes in horizontal cutting for different tool path linking methods: (a) one way, (b) zig-zag

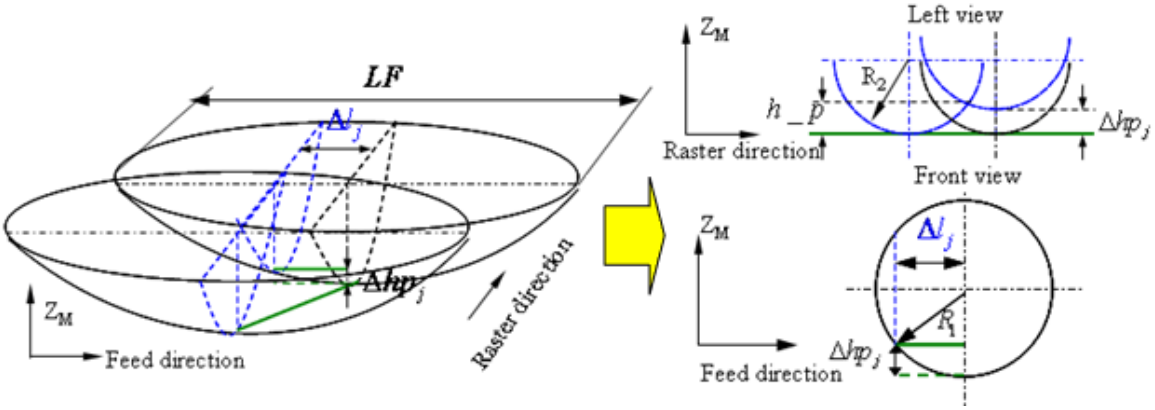

Figure 6. Generation of shift height in raster direction due to the existence of shift length

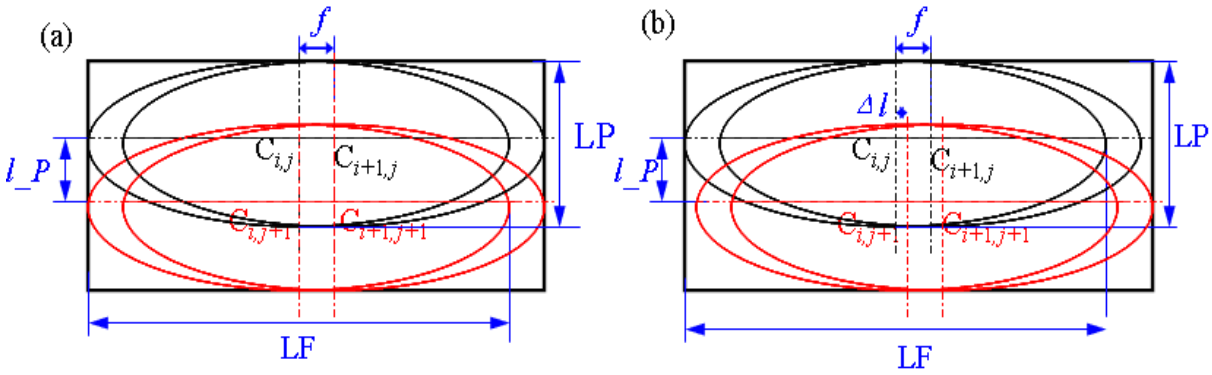

Figure 7. Surface topography patterns under small values of feeding length and path-interval: (a) in the absence of shift length; (b) in the existence of shift length

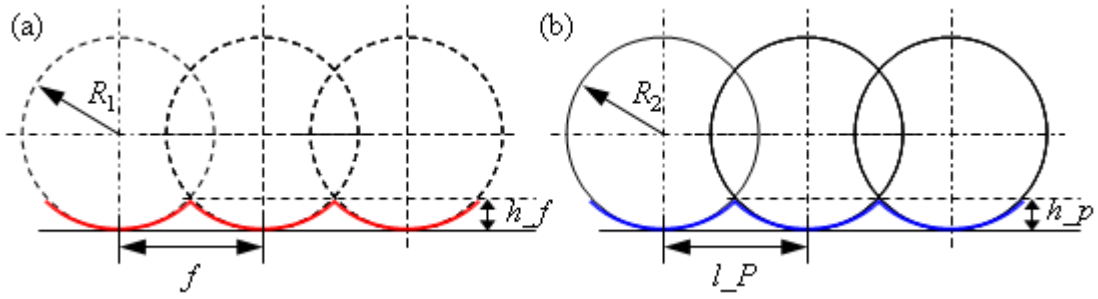

Figure 8. The theoretical scallop height calculation model (a) in feed direction, (b) in raster direction

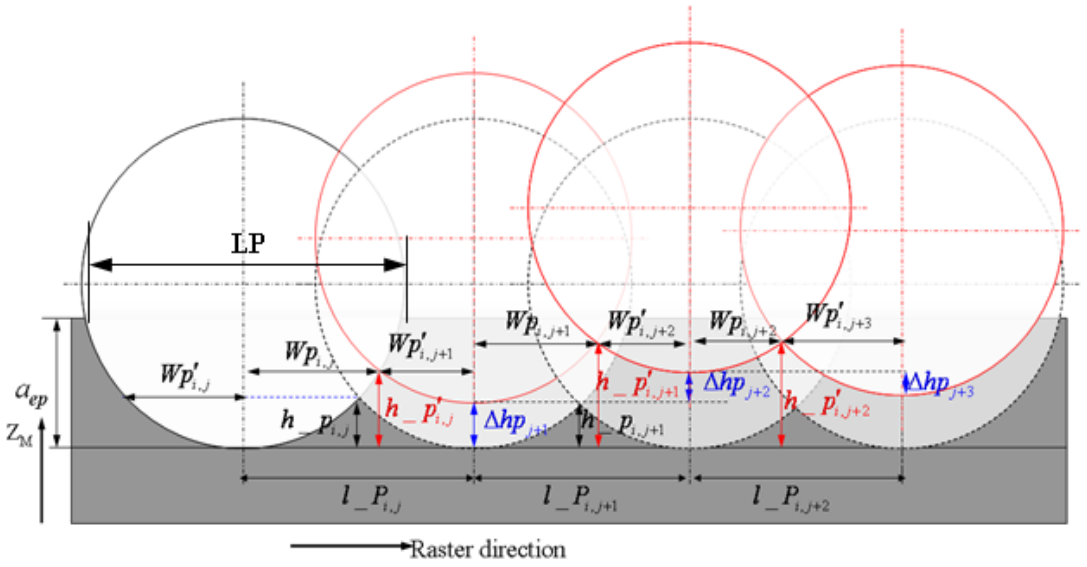

Figure 9. Effects of shift length on path-interval scallop height without tool-interference

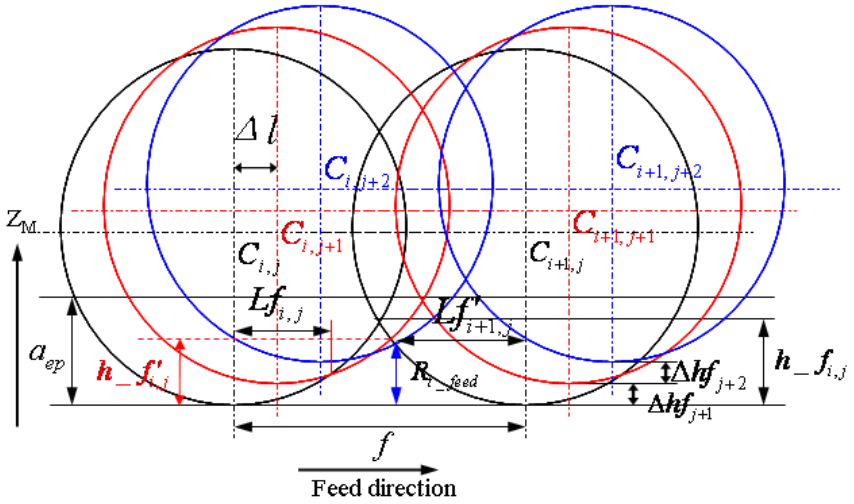

Figure 10. Effect of tool-interference on feed-interval scallop height generation

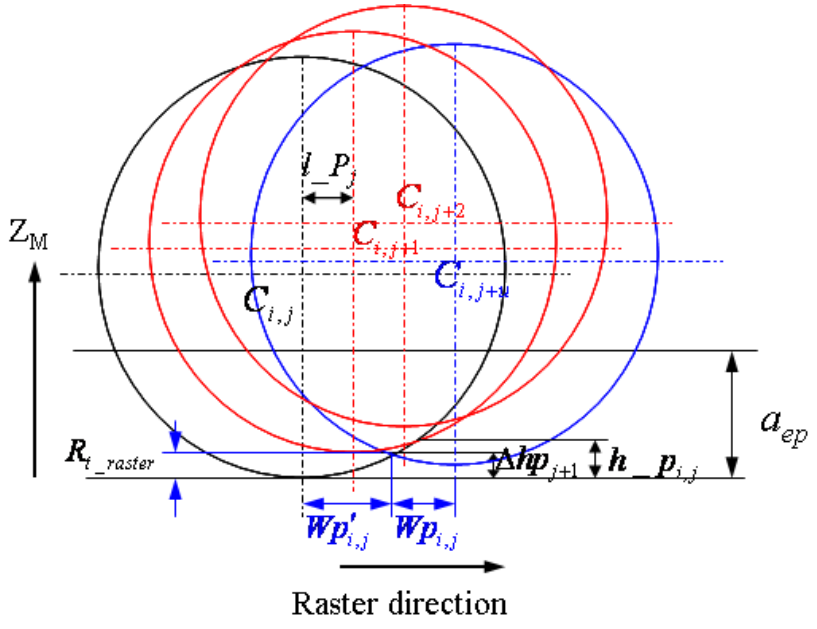

Figure 11. Effect of tool-interference on the path-interval scallop height generation

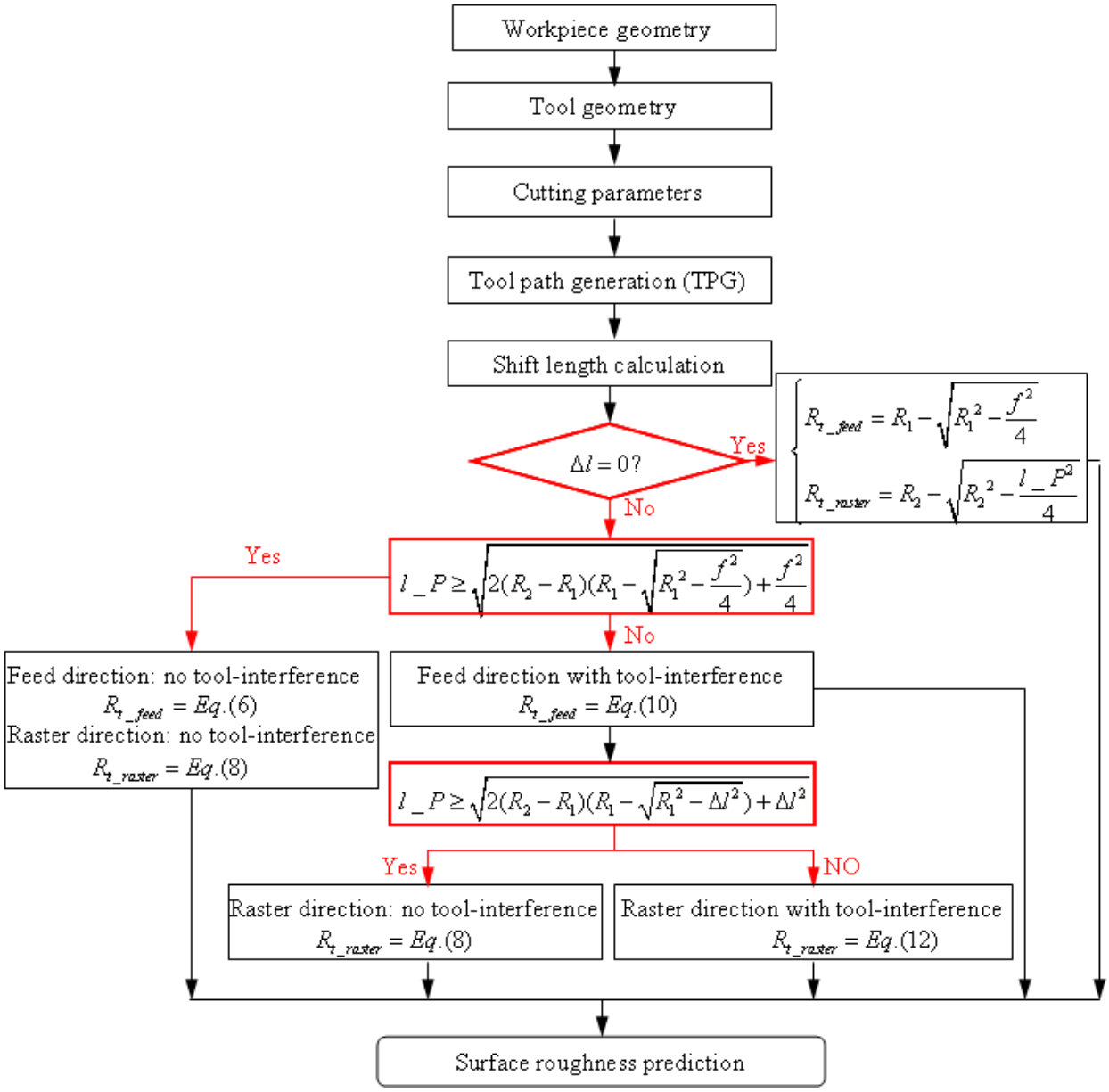

Figure12. Flow chart of calculating the PV heights in UPRM

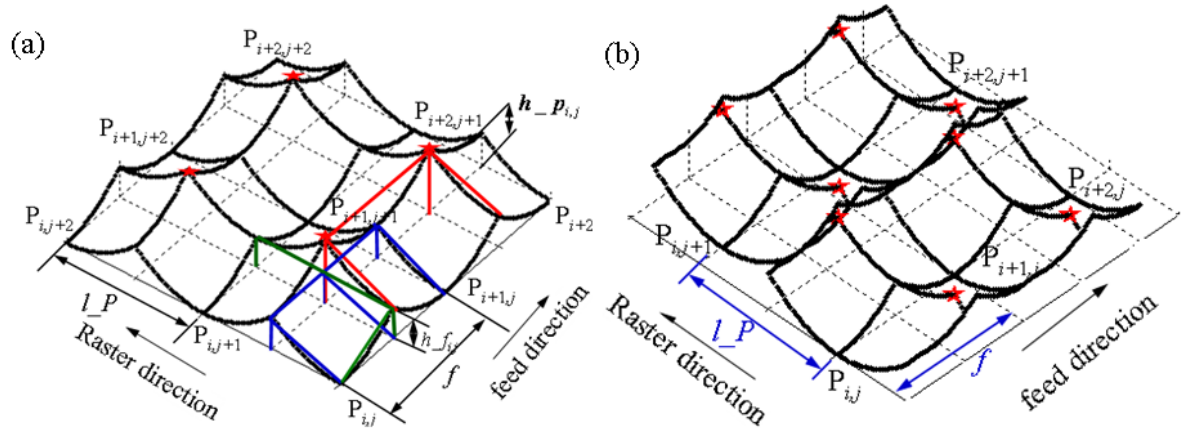

Figure13. The 3D surface roughness prediction model for (a) the absence of shift length; (b) the

existence of shift length

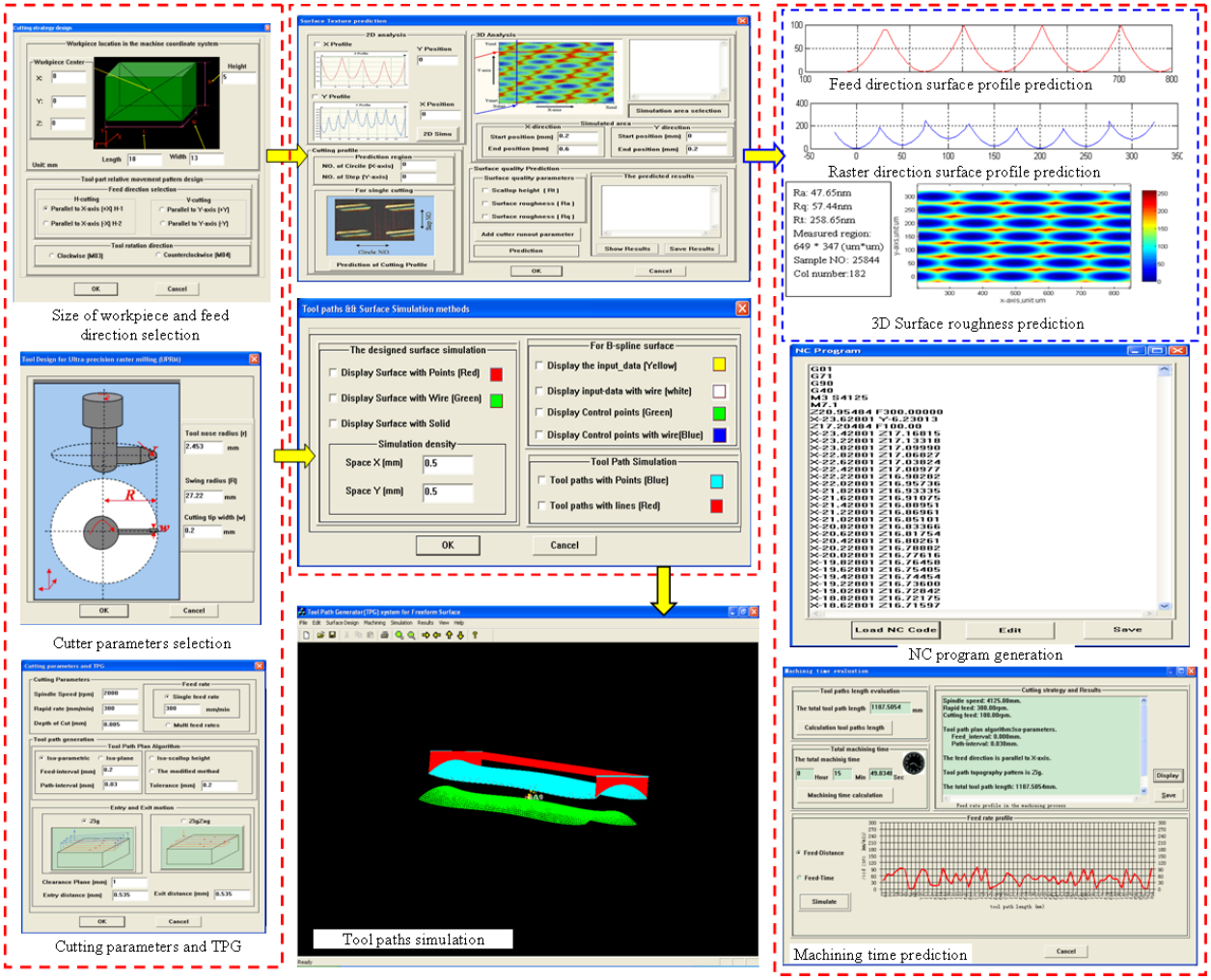

Figure 14.Flow chart of the integrated system for UPRM

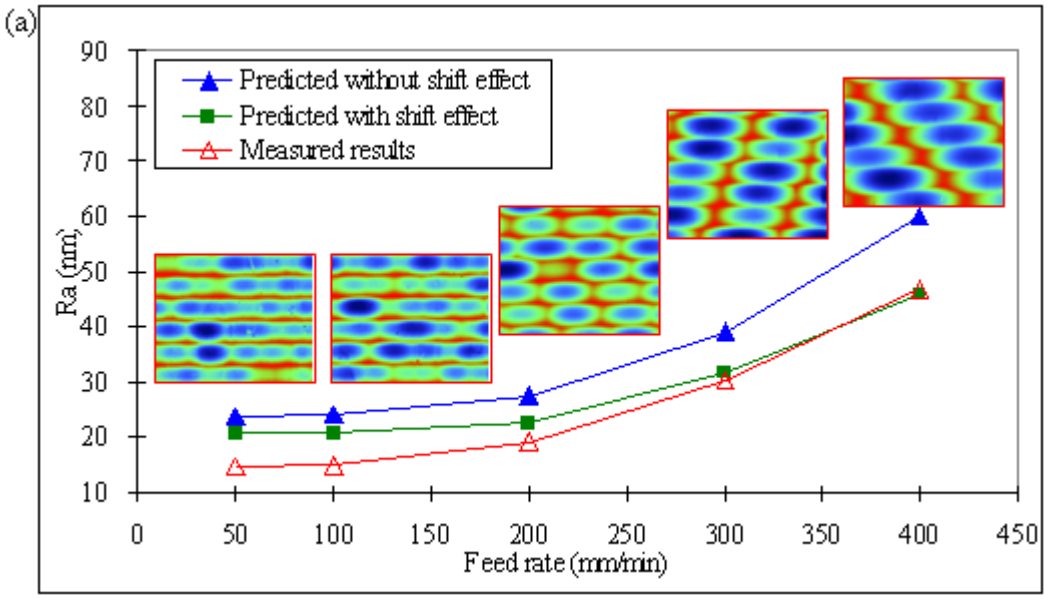

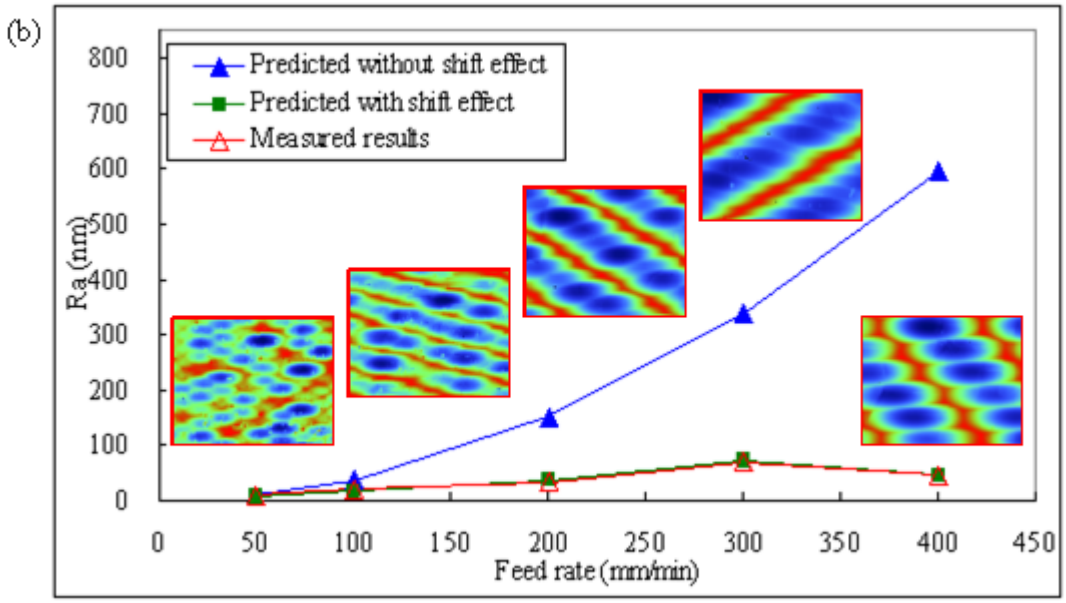

Figure 15. Effects of cutting feed rate on the arithmetical mean roughness (R_a) in: (a) horizontal cutting; (b) vertical cutting

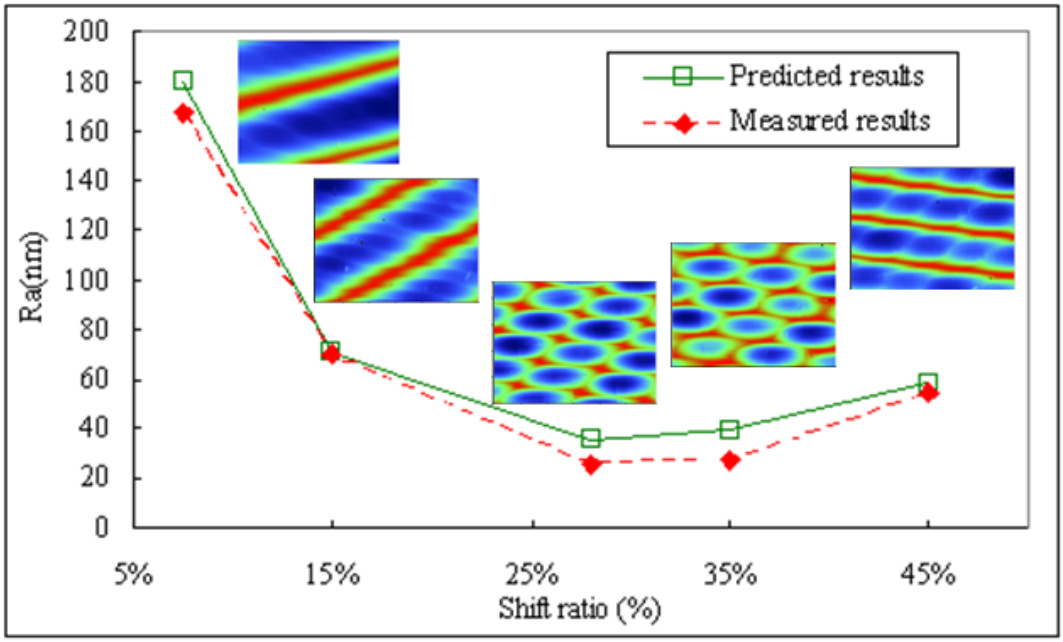

Figure16. Effects of shift ratio on surface roughness (R_a) in vertical cutting

Table 1. Cutting parameters and the geometrical parameters of the tool

Tool parameters		Cutting parameters					Tool path generation		
Tool nose radius (mm)	Swing radius (mm)	Depth of cut (mm)	Spindle speed (rpm)	Cutting feed rate (mm min^{-1})	Rapid feed (mm min^{-1})	Path-interval (mm)	Clearance height (mm)	Entry distance (mm)	Tool path linking method
1.8	27.07	0.005	2000	400, 300, 200,100, 50	300	0.04	1.5	0.8	one way